

Human α -fetoprotein as a Zn^{2+} -binding protein. Tight cation binding is not accompanied by global changes in protein structure and stability

Serge E. Permyakov ^a, Keith A. Oberg ^b, Alexandra M. Cherskaya ^a,
Mikhail M. Shavlovsky ^c, Eugene A. Permyakov ^a, Vladimir N. Uversky ^{a,b,*}

^a Institute for Biological Instrumentation, Russian Academy of Sciences, 142292, Pushchino, Moscow Region, Russia

^b Department of Chemistry and Biochemistry, University of California, Santa Cruz, CA 95064, USA

^c Institute of Experimental Medicine, Russian Academy of Medical Sciences, St. Petersburg, Russia

Received 25 May 2001; received in revised form 7 August 2001; accepted 30 August 2001

Abstract

The binding of zinc to human α -fetoprotein (AFP) isolated from human umbilical cord serum was studied by fluorimetric Zn^{2+} -titration. We found that the total number of strong binding sites for zinc on this protein was 5: AFP has one very strong (dissociation constant, $K_d < 10^{-8}$ M) and at least four lower affinity zinc binding sites ($K_d < 10^{-5}$ M). Fourier transform infrared (FTIR) analysis revealed that aspartate and histidine residues could be involved in the strong coordination of zinc. Intriguingly, binding of zinc to the protein does not induce structural changes that can be detected by circular dichroism, FTIR, intrinsic fluorescence or (1,1')-bi-(4-anilino)naphthalene-5,5'-disulfonic acid (bis-ANS) binding. Finally, scanning microcalorimetry measurements showed that stability of the protein is also unaffected by zinc binding in spite of the strength of the coordination. Such strong interactions without major structural consequences are highly unusual, and AFP may therefore be the first characterized representative of a new class of ligand-binding proteins. © 2002 Elsevier Science B.V. All rights reserved.

Keywords: α -Fetoprotein; Carcinoembryonic protein; Protein structure; Structural transition; Conformational stability; Zn^{2+} binding

1. Introduction

α -Fetoprotein (AFP) is an oncofetal glycoprotein consisting of 590 amino acid residues [1] that is produced primarily by fetal liver and yolk sack cells. AFP levels correlate with fetal maturity, being very

high during embryo development and decreasing abruptly just after birth. An increase in the AFP content in adult sera is evidence of the development of several disorders [2].

AFP is a well-known molecular marker indicating either the development of cancer or fetal abnormalities [2–9]. In addition to its substantial diagnostic importance, the physiological functions of AFP are also of great interest. It has been established that AFP isolated from amniotic fluid or the fetal sera of rats is capable of binding estrogens [9–12]. It was shown that AFP strongly binds to fatty acids [9,13,14] – material isolated from human fetuses contains from 2–3 molecules of fatty acid per protein

* Corresponding author. Present address: Department of Chemistry and Biochemistry, University of California, Santa Cruz, CA 95064, USA. Fax: +1-831-459-2935.

E-mail address: uversky@hydrogen.ucsc.edu (V.N. Uversky).

molecule, (mainly unsaturated: arachidonic – C20:4 – and docosahexaenoic – C22:6 – acids). Human hepatoma AFP isolates have a much larger variety of bound fatty acid than fetal isolates [13,15]. A single high-affinity binding site for bilirubin has also been demonstrated [14,16]. In addition to its transport function, AFP plays a role in the regulation of cell division and metabolism and modulates the behavior of microphages [17] and T-lymphocytes [18]. A role for AFP in the suppression of the immune response has also been suggested [9,17,19].

It is known that AFP and human serum albumin (HSA) have considerable structural similarity [1,21,22,26,27] and interact with the same organic ligands; for this reason AFP is often regarded as a fetal-type albumin [9]. There are, however, differences between the binding properties of these two proteins – the number of different ligands transported by HSA is much larger than that of AFP. Additionally, albumin's affinity for many organic ligands is in the range of dissociation constant $K_d = 10^{-6}$ – 10^{-4} M, while for AFP the binding is considerably stronger ($K_d = 10^{-8}$ – 10^{-6} M) [9]. Natural ligands play an important role in stabilizing the native tertiary structure of AFP [20–25]. The complete removal all ligands transforms AFP into a molten globule-like conformation [21–23]. In contrast, release of ligands from HSA causes only a minor decrease in its stability [21,28].

Although for HSA the formation of stable complexes with Ca^{2+} [29]; Cu^{2+} and Ni^{2+} [30,31]; Zn^{2+} [32]; Mg^{2+} , Co^{2+} and Cd^{2+} [33] and many other metal cations has been established [34], little is currently known about the interaction of AFP with metal ions. The presence of high-affinity binding sites for copper and nickel on human AFP has been observed [35], and its interaction with several heavy metals (including zinc and lead) has been studied by gel-filtration chromatography [36]. This method is known to give reasonable estimates of the dissociation constants in the micromolar range. AFP was shown to be capable of binding to a total of ~ 16 Zn^{2+} ions. Of these, 4–5 bind to high-affinity sites with dissociation constants on the order of $K_d = 6$ – 8×10^{-6} M [36]. The K_d estimates for low-affinity sites were less certain, and the structural effects of zinc binding to AFP were not explored.

Zinc is essential for the normal function of most

organisms and it has been shown to be a required cofactor in a variety of biochemical processes in plants, bacteria and higher organisms [37–39]. Zinc is particularly important for fetal growth in vertebrates [39]. The concentration of this metal in living cells is high – it is second only to iron among the transition elements. It is therefore not surprising that Zn^{2+} deficiency causes several pathological disorders [39]. Zinc ions are key structural components in a large number of proteins, and are essential for catalytic activity. The list of zinc-binding and zinc-activated proteins includes, for example, DNA and RNA polymerases, carboxypeptidases, alcohol dehydrogenase, phospholipases and many others [39].

In the following paragraphs we present the results of a spectroscopic study that characterizes the structure of human AFP and its interaction with Zn^{2+} . The primary Zn^{2+} titration data are based on cation-induced changes in protein fluorescence parameters. This approach allows precise measurements within a wide range of dissociation constant values. To supplement this data, we present circular dichroism (CD), Fourier transform infrared (FTIR), calorimetric and fluorescence data that characterize the effect of zinc on the secondary and tertiary structure of AFP as well as its stability, solvent accessibility and hydrophobicity.

2. Materials and methods

2.1. Protein isolation

The protein was isolated from human umbilical cord serum by chromatographic and immunoaffinity methods. The major contaminant proteins were removed by a series of chromatographic steps including DEAE–Sephadex, DEAE–Sephacrose, KM–Sephacrose, Cibacron Blue–Sephacrose and protein G–Sephacrose columns. The final stages of AFP purification were carried out on immunoaffinity columns with immunosorbents saturated with antibodies against impurity proteins. The purity of AFP was no less than 98%, as measured by sodium dodecyl sulfate and native polyacrylamide gel electrophoresis. Apo-form of AFP was prepared according to Blum et al. [40].

2.2. Materials

Buffer compounds and analytical or extra pure grade urea were used without additional purification. Zinc-titration experiments were performed in 10 mM HEPES buffer, pH 8.0. Calorimetric measurements were carried out in 50 mM cacodylate buffer, pH 6.88. The buffer system for FTIR and CD measurements was 100 mM sodium phosphate, 0.15 M NaCl, pH 7.2.

2.3. Spectroscopic measurements

Protein concentrations were determined by the absorbance at 280 nm using extinction coefficient of $\epsilon_{1\text{ cm}^2, 280\text{ nm}}^{1\text{ mg/ml}}$ and 0.455 for AFP and bovine serum albumin (BSA), respectively. For circular dichroism (CD), infrared and calorimetric measurements the protein concentration was 0.5–1.0 mg/ml, while fluorescence measurements used 0.01 mg/ml protein solutions.

CD spectra were collected on an AVIV-60DS spectropolarimeter, equipped with a temperature-controlled cell-holder. The cell path lengths were 0.1 and 10.0 mm for far and near UV CD measurements, respectively. Trp and (1,1')-bi-(4-anilino)naphthalene-5,5'-disulfonic acid (bis-ANS) fluorescence were measured with a Jobin Yvon-Spex FluoroMax-2 fluorimeter with excitation at 296 or 350 nm, respectively. Acrylamide quenching studies were performed by adding aliquots from a stock acrylamide solution to a cuvette containing protein solution. Fluorescence intensities were corrected for dilution effects. Fluorescence quenching data were analyzed using the general form of the Stern–Volmer equation, which explicitly models both dynamic and static quenching [41]:

$$\frac{I_0}{I} = (1 + K_{SV}[Q])e^{V[Q]}$$

where I_0 and I are the fluorescence intensities in the absence and presence of quencher, respectively; K_{SV} is the dynamic quenching constant; V is a static quenching constant; $[Q]$ is the concentration of the quencher.

2.4. Attenuated total reflection (ATR)-FTIR spectra

ATR-FTIR spectra were collected on an air-purged Nicolet 800SX spectrometer equipped with

an N₂(l)-cooled MCT detector [42]. Sample solutions were applied to the surface of a 72 × 10 × 6 mm, 45° trapezoidal germanium internal reflection element (IRE), and the bulk solvent was evaporated under a gentle stream of nitrogen gas. One hundred and twenty-eight scans were accumulated for each sample at a resolution of 4 cm⁻¹. Interferograms were transferred to a Windows PC, and processed with GRAMS/32 (Galactic Industries) and the SAFAIR software package (America's Solutions Providers, Orlando, FL). Fourier transformation used the Mertz method with medium Norton–Beer apodization. Absorbance spectra were generated using the spectrum of the clean IRE as a reference. Water vapor signal was subtracted based on the area of the 1712 peak during the generation of absorbance spectra. Minor imprecision in this subtraction was corrected during the optimization of subsequent subtraction steps by simultaneous vapor-subtraction. Secondary structure determination was performed using a partial least-squares analysis (PLSplus for GRAMS/32) with the RaSP50 protein reference set [43,44]. For the analyses, IR and CD data were combined into a single 'hybrid' spectrum (K.A. Oberg, J.M. Ruyschaert, E. Goormaghtigh, unpublished data).

α -Fetoprotein samples were 80 μ l of 1 mg/ml solution in 1 mM HEPES buffer (pH 8.0) with or without a 10-fold molar excess of zinc (ZnCl₂). Bovine serum albumin (Sigma B1900) was prepared as a 10 mg/ml solution in ddH₂O (150 μ M); 20 μ l was applied to the IRE surface for each sample, with or without a 13-fold molar excess of zinc (a 130-fold excess was examined also). Amino acid solutions of glycine, aspartic acid, glutamic acid, and histidine HCl (Sigma) were prepared by dissolving each compound in water to a final concentration of 100 mM; one equivalent of NaOH was added to each solution except glycine. These solutions were then diluted into five volumes of ddH₂O or 100 mM zinc chloride; 20 μ l of this final solution was used to prepare a thin film for ATR in the manner described above. Finally, two spectra of zinc chloride were collected under atmospheres with different water vapor content.

There is evidence of a substantial amount of bound water in the ATR-FTIR spectrum of a zinc chloride thin film (Fig. 5). Bands at 3425, 2006, and 1619 cm⁻¹ show the intensity pattern characteristic of water, but with offset frequencies, which is indica-

tive of substantial interaction with the hygroscopic salt. By using a large excess of zinc chloride in each of the ATR films, conditions were such that this signal and any other characteristics of zinc chloride dominated the spectrum and could therefore be removed by subtraction of the pure ZnCl_2 film spectrum. Extraction of amino acid spectra was performed by iteratively optimizing a subtraction scaling factor to give a linear baseline in the $1900\text{--}1700\text{ cm}^{-1}$ region with the SAFAIR 'linear' function. This approach removed the hydrated ZnCl_2 signal from the total spectrum without over subtracting.

2.5. Calorimetric measurements

Calorimetric measurements were made with a DASM-4M scanning microcalorimeter (Institute for Biological Instrumentation of the Russian Academy of Sciences, Pushchino, Moscow Region, Russia). The rate of heating was 1 K/min. The excess pressure was kept at 3.6 atm. The excess heat capacity of AFP was determined as described elsewhere [45].

3. Results

3.1. The secondary structure of AFP and SA

Fig. 1 compares far UV CD and FTIR spectra of

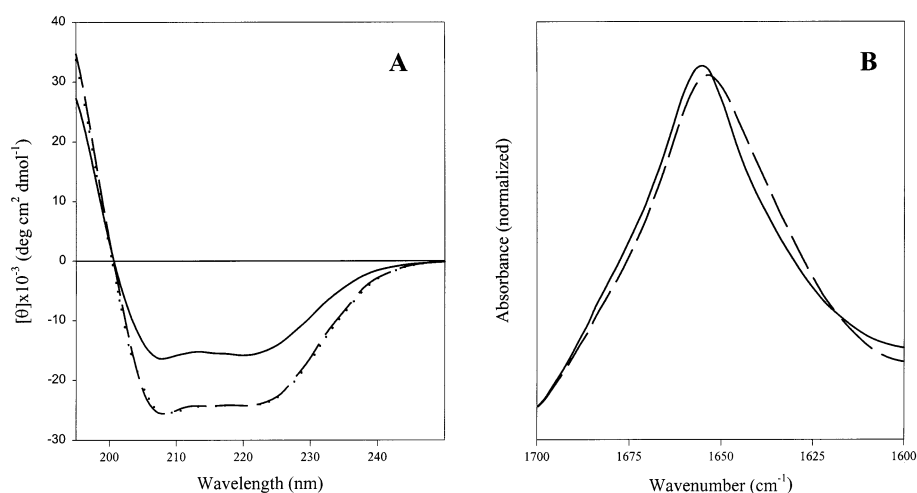


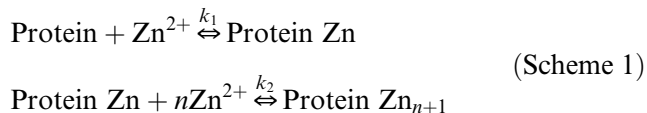
Fig. 1. Far UV CD (A) and FTIR (B) spectra of AFP (solid line) and BSA (dashed line) measured under conditions of 100 mM sodium phosphate buffer (pH 7.2), 0.15 M NaCl. Far UV CD spectrum of HSA is shown for comparison (dotted line). The protein concentration was 0.5 and 1.0 mg/ml for CD and FTIR measurements, respectively. Cell with pathlength of 0.1 mm was used in far UV CD spectra measurements.

two homologous proteins, AFP and BSA. The far UV CD spectrum of HSA is also present for comparison. One can see that HSA and BSA have completely superimposable spectra, reflecting the essentially identical structure of these proteins. Fig. 1A demonstrates also that far UV CD spectrum of AFP is very different from spectra of both serum albumins. However, Fig. 1B shows that the IR spectra of AFP and BSA have a similar appearance, with sharp symmetrical peaks at 1656 and 1545 cm^{-1} which are characteristic of all- α proteins. The results of quantitative secondary structure analyses of the spectra with the RaSP50 reference set [43,44] are shown in Table 1. Analysis of hybrid IR-CD spectrum ([46]; K.A. Oberg, J.M. Ruyschaert, E. Goormaghtigh, unpublished data) allows us to estimate that the helix content is in fact, quite high for AFP, being comparable to the globins or 4-helix bundle proteins [44].

3.2. Spectrofluorimetric titration of AFP with Zn^{2+}

The fluorescence results from Zn^{2+} -titration of AFP are shown in Fig. 2A. The increase in Zn^{2+} concentration results in a small blue shift of the intrinsic tryptophan fluorescence spectrum and a decrease in fluorescence quantum yield (see inset to Fig. 2A). Fig. 2A shows that the spectral changes proceed in two distinct steps. The first stage corre-

sponds to the strong binding of one Zn^{2+} per protein molecule, while the second step is due to the cooperative binding of several additional Zn^{2+} ions to the zinc-loaded protein (Scheme 1):



The Zn^{2+} -induced changes in Trp fluorescence intensity were fit according to the Scheme 1. The fit was optimized by varying the number of zinc cations bound, n , and the binding constant values k_1 and k_2 . The best fit was achieved when $k_1 = 1.0 \times 10^9 \text{ M}^{-1}$, $k_2 = 1.1 \times 10^5 \text{ M}^{-1}$ and $n = 4.1$. Interestingly, Fig. 2A shows that the titration results are independent of the nature of anion (Cl^- or SO_4^{2-}) assuming that the observed effects are definitely due to the Zn^{2+} binding.

Similar results were obtained when zinc-AFP binding was monitored by changes in bis-ANS fluorescence (Fig. 2B), which shows that increasing the Zn^{2+} concentration caused a blue shift of the bis-ANS fluorescence spectrum maximum and an increase in its intensity. It can also be seen that bis-ANS fluorescence is affected by the binding of Zn^{2+} to both the strong site and the weaker secondary sites, although binding to the strong site produces a much smaller change in fluorescence. Fits of the fluorescence intensity at 440 nm gave $k_1 \sim 1 \times 10^9 \text{ M}^{-1}$, $k_2 = 1.1 \times 10^5 \text{ M}^{-1}$ and $n = 2.5$. Note that these estimates of the binding parameters, based on the properties of an extrinsic probe, agree well with the parameters determined using the intrinsic fluorescence of AFP.

The very tight association of zinc with AFP brought up the question of possible structural con-

sequences of the interaction. It is known that natural ligands often play an important role in stabilizing protein structure [47]. It has been demonstrated that complete release of organic ligands transforms AFP into a molten globule-like conformation, i.e., a compact denatured form, with native-like compactness and secondary structure content but the absence of rigid tertiary structure [21–23].

3.3. Effect of zinc binding on structural properties of AFP

The data presented in the inset to Fig. 2A are consistent with the suggestion that the interaction of AFP with zinc induces some changes in the environment of tryptophan. To further probe such changes we investigated the acrylamide quenching of Trp fluorescence. Fig. 3 shows the upward curvature of the Stern–Volmer plots obtained from these measurements; this is characteristic of both dynamic and static quenching. The data were analyzed according to the general form of the Stern–Volmer equation (see Section 2). There was a slightly less pronounced effect in the zinc-loaded protein than there was with AFP in the absence of Zn^{2+} . K_{SV} was $6.14 \pm 0.08 \text{ M}^{-1}$ when no zinc was present, whereas $K_{\text{SV}} = 5.82 \pm 0.05$ and $5.35 \pm 0.07 \text{ M}^{-1}$ for $[\text{Zn}^{2+}]/[\text{AFP}] = 1.0$ and 10, respectively. This suggests that the accessibility of Trp decreases as zinc binds to the protein. In Fig. 4, we present near (A) and far UV CD spectra of AFP (B) with different zinc concentrations. It can be seen that addition of Zn^{2+} to AFP solutions induces only minor changes in the near UV CD spectrum. This indicates that the degree of asymmetry of the environment of aromatic amino acid residues is essentially unaltered by zinc coordination. The absence of changes in

Table 1
Results from RaSP analysis of AFP and serum albumin

Structure	CD			IR			IRCD hybrid		
	AFP	BSA	SECV	AFP	BSA	SECV	AFP	BSA	SECV
α -helix	53.1	69.8	8.1	64.4	48.7	8.5	60.4	61.5	6.7
β -sheet	6.2	0	11.6	0	2.4	7.7	0	0	7.9
Turn	11.3	10.9	4.5	13.7	14.3	4.1	11.3	10.9	4.4
Remainder	29.1	30.5	9.8	30.6	37.2	11.1	30.9	30.7	9.6

Values in the table represent the percentage of each structure found by the analysis.

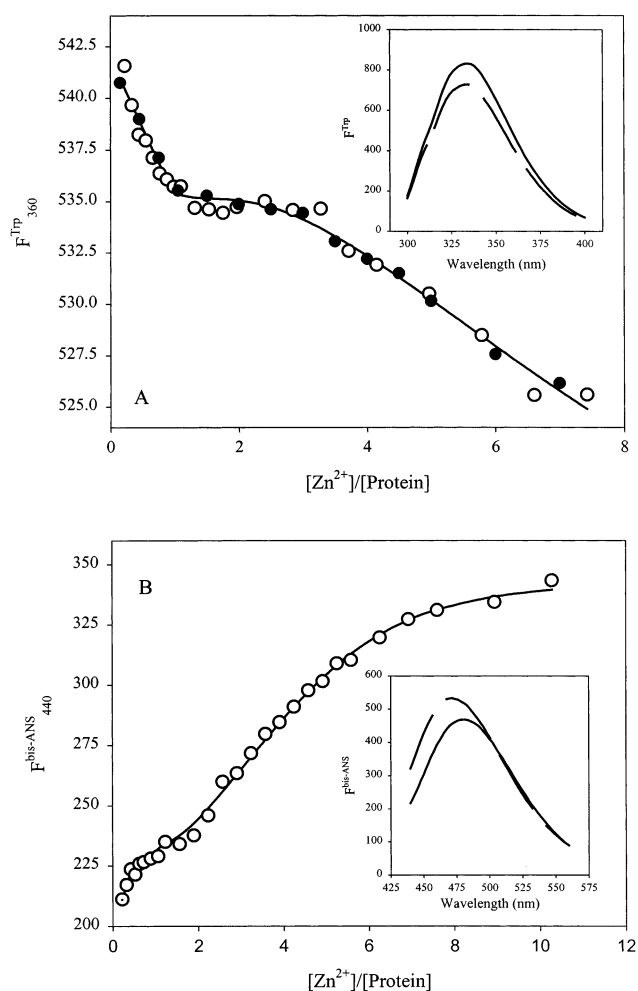


Fig. 2. Spectrofluorometric Zn^{2+} -titration of AFP monitored by changes in intrinsic fluorescence intensity at 360 nm (A) or fluorescence intensity of bis-ANS at 440 nm (B). Open and closed symbols in A correspond to the AFP titration by $ZnCl_2$ and $ZnSO_4$, respectively. Solid lines in both panels represent fits of the experimental data according to Scheme 1 (see text). The fits were optimized by varying the number of zinc cations bound, n , and the binding constant values k_1 and k_2 . The best fit was achieved when $k_1 = 1.0 \times 10^9 \text{ M}^{-1}$, $k_2 = 1.1 \times 10^5 \text{ M}^{-1}$ ($n = 4.1$) and $k_1 = 0.9 \times 10^9 \text{ M}^{-1}$, $k_2 = 1.1 \times 10^5 \text{ M}^{-1}$ ($n = 2.5$) for the intrinsic fluorescence intensity and bis-ANS fluorescence intensity, respectively. Insets represent corresponding spectra measured in the absence (solid lines) or in the presence (dashed lines) of Zn^{2+} ($[Zn^{2+}]/[Protein] = 10:1$). Trp and bis-ANS fluorescence was excited at 296 or 350 nm, respectively. Measurements were carried out in 10 mM HEPES buffer (pH 8.0) at 25°C. Protein concentration was 0.01 mg/ml, whereas bis-ANS concentration was 0.1 μM .

the far UV CD spectra of AFP (Fig. 4B) shows that secondary structure of AFP is not changed by zinc binding.

These results are supported by the FTIR spectra of zinc-free and zinc-loaded AFP. Fig. 5 shows that only subtle changes were induced in the infrared spectrum of AFP by complexation with $ZnCl_2$. In particular, a reproducible narrowing of the amide I and II bands was observed which is indicative of either a slight increase ($\leq 5\%$) in the amount of α -helix in the protein or possibly a decrease in the conformational sampling of the protein, i.e., an increase in rigidity. A subtle narrowing was also observed in the IR spectrum of BSA in the presence of $ZnCl_2$, which is consistent with the well-known similarity of these two proteins (Fig. 5).

In contrast to this similarity, a prominent new band appeared at 1592 cm^{-1} with AFP in the presence of $ZnCl_2$. As shown in Fig. 5, the band clearly does not arise from zinc chloride alone. To identify the group responsible for the band, ATR-FTIR spectra of several amino acids were collected (Fig. 5) in the presence and absence of an excess of $ZnCl_2$. Of these, only aspartic acid exhibited a $ZnCl_2$ -induced band that matched the frequency observed in the protein spectrum. This allows us to hypothesize that aspartate residues are involved in the coordina-

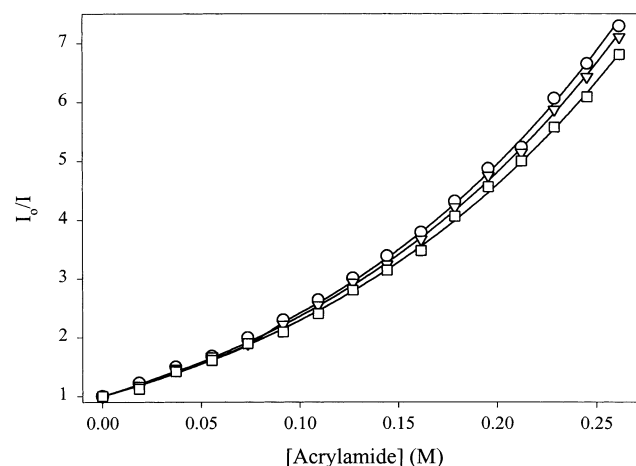


Fig. 3. Stern-Volmer plots for acrylamide quenching of AFP tryptophan fluorescence under conditions of different excess of Zn^{2+} : no zinc added (\circ), $[Zn^{2+}]/[AFP] = 1.0$ (∇) and $[Zn^{2+}]/[AFP] = 10$ (\square). Measurements were carried out in 10 mM HEPES buffer (pH 8.0) at 25°C. Protein concentration was kept around 0.01 mg/ml.

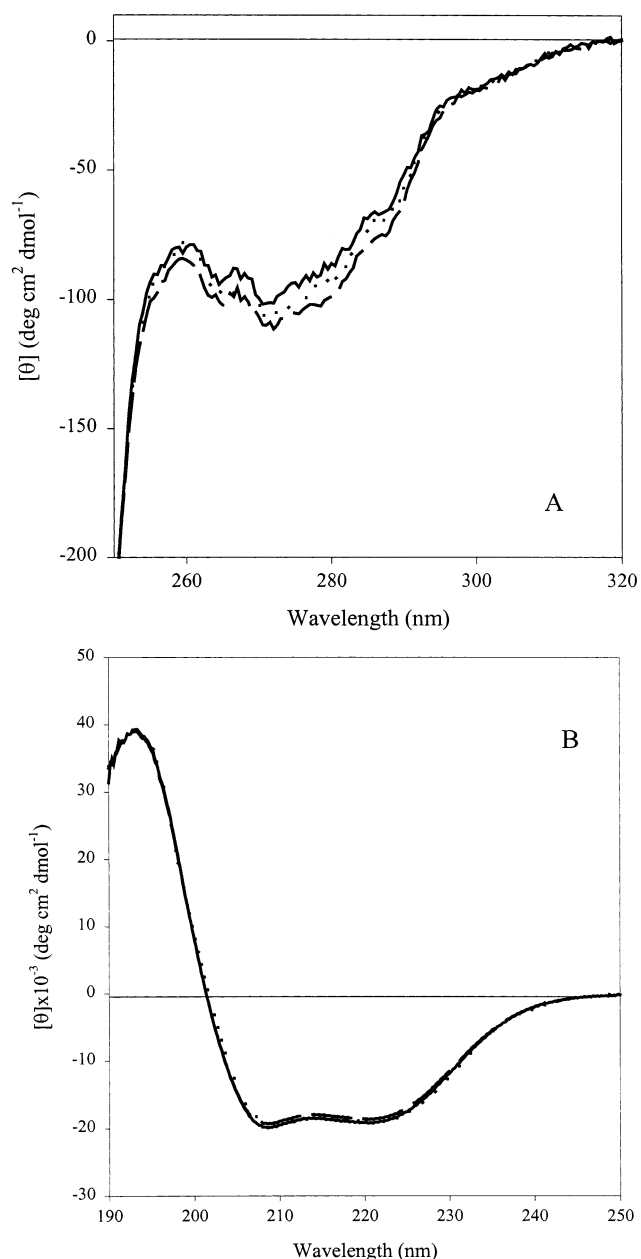


Fig. 4. Effect of zinc binding on near (A) and far UV CD spectra of AFP (B). Spectra were collected under conditions of different excess of Zn^{2+} : no zinc added (solid lines), $[\text{Zn}^{2+}]/[\text{AFP}] = 1.0$ (dotted lines) and $[\text{Zn}^{2+}]/[\text{AFP}] = 10$ (dashed lines). Protein concentration was 0.5 and 1.0 mg/ml whereas cell path-length was 10 and 0.1 mm for near and far UV CD spectra measurements, respectively.

tion of zinc. However, we cannot exclude that His residues also contribute to Zn^{2+} binding, as there is some enhancement in the intensity of the band with frequency $\sim 1590 \text{ cm}^{-1}$ (see Fig. 5).

3.4. Conformational stability of Zn^{2+} -free and Zn^{2+} -loaded AFP

Results of the conformational stability analysis are presented in Fig. 6. Calorimetric curves were measured for zinc-free and zinc-loaded AFP ($[\text{Zn}^{2+}]/[\text{AFP}] = 1.0$ and 10). It can be seen that stability of the protein is not significantly affected by the filling

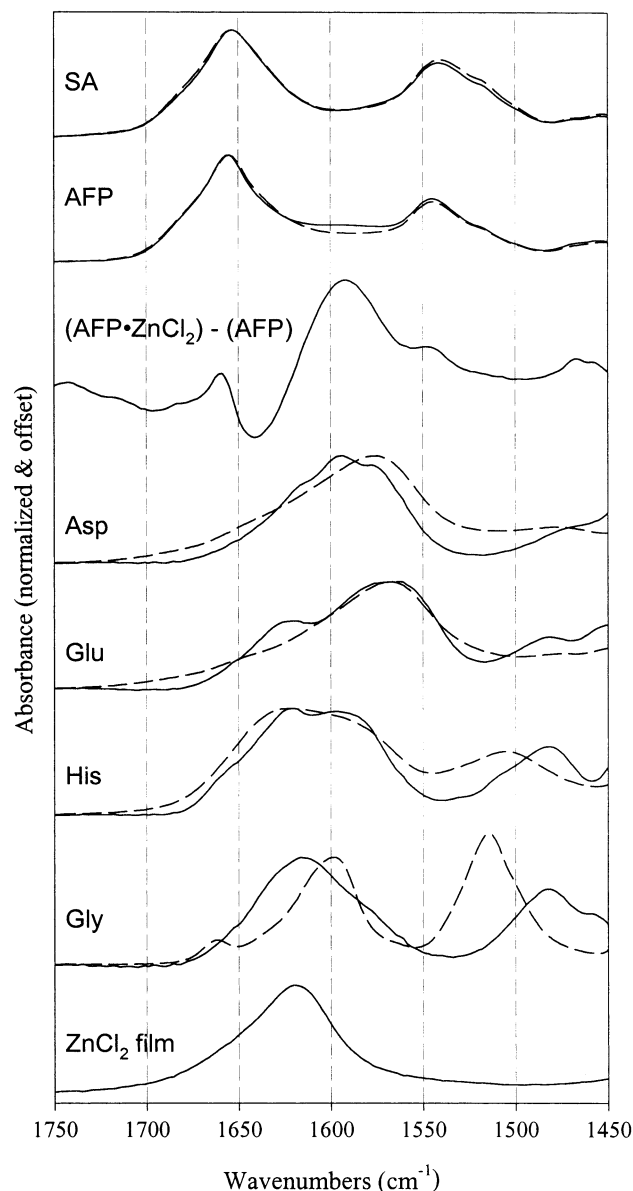


Fig. 5. Effect of zinc binding on FTIR spectra of AFP, BSA and several individual amino acid residues (Asp, Glu, His and Gly). Spectra of zinc-free and zinc-loaded samples are shown by dashed and solid lines, respectively. See Section 2 for details of experiments.

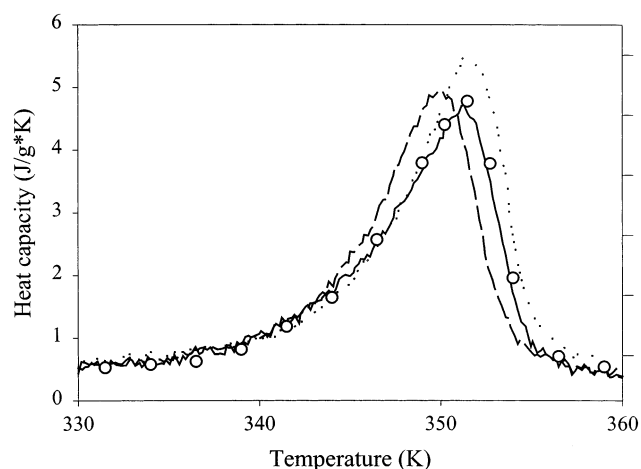


Fig. 6. Calorimetric curves for zinc-free and zinc-loaded AFP. Measurements were done under conditions of different excess of Zn^{2+} : no zinc added (solid lines), $[Zn^{2+}]/[AFP]=1.0$ (dotted lines) and $[Zn^{2+}]/[AFP]=10$ (dashed lines). Measurements were carried out in 50 mM cacodylate buffer, pH 6.88. Protein concentration was 1 mg/ml. Open circles correspond to the AFP melting in 50 mM cacodylate buffer (pH 7.0) in the presence of 150 mM NaCl.

of the strong zinc-binding site ($[Zn^{2+}]/[AFP]=1.0$), whereas the binding of additional zinc ions causes some decrease in protein stability. The data presented in Fig. 6 show that the T_m of AFP is shifted downward by $\sim 2^\circ C$ when a 10-fold molar excess of zinc is present.

It is known that chloride ion may destabilize the protein structure [48]. To exclude this possibility, AFP thermal stability in the presence of 150 mM NaCl was studied. Fig. 6 shows that the addition of large excess of this anion ($[Cl^-]/[AFP]=10\,000$) was not accompanied by any detectable changes in the AFP thermal stability, underlining the destabilization role of Zn^{2+} binding.

4. Discussion

The data obtained in this study show that AFP has a structure similar to SA and at least five strong zinc-binding sites. One of these is characterized by a dissociation constant $K_d \sim 10^{-9}$ M, whereas four others have a lower affinity ($K_d \sim 10^{-5}$ M). Earlier gel-filtration [36] data suggested that AFP has four to five high-affinity zinc-binding sites with a dissoci-

ation constant of $K_d = 6\text{--}8 \times 10^{-6}$ M. These binding parameters are similar to those measured here for the weaker sites ($n=4$, $K_d = 10 \times 10^{-6}$ M). However, we were able to identify a previously undetected very strong zinc binding site ($K_d \sim 10^{-9}$ M) using fluorescent titration. The advantage of this technique lies in its sensitivity to changes in the spectral properties of the protein or fluorescent dye induced by ligand binding. More importantly, it allows extraction the reliable information on very strong interactions if the binding of ligand to the protein reproducibly induces changes in the protein fluorescence parameters [49].

In addition, the application of FTIR has allowed us to extract information on residues that may be involved in the strong binding of zinc to AFP. Comparison of FTIR spectra for bound and unbound AFP reveals a new band at 1592 cm^{-1} that results from zinc coordination by side chains. Comparison of this change with IR spectra of model compounds has allowed us to tentatively identify the group(s) responsible for this new band. We have established that the FTIR spectrum of zinc-loaded aspartate has a new band at the frequency observed in the spectrum of zinc-bound AFP. Additionally, some enhancement of the band in the vicinity of 1590 cm^{-1} has been observed for zinc-loaded histidine (see Fig. 5). Thus, aspartate (and, probably, histidines) may be responsible for the strong coordination of zinc by AFP. In spite of the strong similarity between the amide I and II spectra of these proteins, the same band was not observed in the FTIR spectrum of zinc-loaded BSA, even in the presence of a 130-fold excess of $ZnCl_2$. It was shown previously that the pK of zinc binding to both AFP and HSA is close to pH 6.0 [36]. This suggests that histidine is involved in zinc binding, since the pK of imidazole is close to neutral [50]. Taken together, all this evidence shows that there is considerable difference in zinc binding by two homologous proteins, AFP and SA. Although histidines are crucial for the binding of zinc by both proteins, aspartate may play an additional important role in the coordination of Zn^{2+} by AFP.

Finally, we have shown here that zinc binding to AFP does not induce significant changes in protein structure or stability. Both the FTIR and CD spectra of AFP indicate that this protein is a member of

the all α class. Partial least-squares analysis with the RaSP reference set [43,44] suggests that the protein has $60\% \pm 7$ α -helix, no β -sheet, and that its secondary structure is not significantly altered by zinc binding. As it follows from intrinsic fluorescence and near UV CD analysis, there are only minor changes in the environment and solvent accessibility of the sole Trp residue caused by zinc binding. In addition, the overall hydrophobicity of AFP increases slightly as a result of zinc binding. This conclusion follows from small zinc-induced increase in bis-ANS fluorescence intensity (inset to Fig. 2B). Calorimetric analysis shows that the stability of the protein is also almost insensitive to Zn^{2+} binding.

These data show that the properties of AFP differ considerably from those of most ligand binding proteins. The effects of natural ligands on the structural properties and conformational stability of globular proteins have been categorized [47]. It was concluded that according to the structural consequences of the ligand release, ligand-binding proteins could be divided into several classes [47].

Class I: release of ligands does not result in noticeable changes of the unique protein structure, but the conformational stability of the protein molecule changes essentially;

Class II: detectable changes of the spatial protein structure are observed in the ligand-free form – however, the protein yet possesses a pronounced tertiary structure;

Class III: in the ligand-free form the tertiary structure completely disappears, the secondary structure is retained, and the protein molecule remains compact;

Class IV: the ligand-free form of the protein has no tertiary structure, the secondary structure content is noticeably less than in the holo-protein, and dimensions of the apo-protein distinctly differ both from coil dimensions and from that of holo-protein;

Class V: the apo-form represents a virtually completely unfolded polypeptide chain.

It was also shown that although the range of possible structural transformations induced in a protein molecule by ligand binding is very wide, a change of global structural properties and/or conformational stability of the proteins are always observed upon ligand binding.

Surprisingly, this is not the case for AFP. Thus this protein represents new class of ligand-binding proteins, for which neither the global structure nor the conformational stability are affected by the very tight binding of the ligand.

References

- [1] T. Morinaga, M. Sakai, G. Wegmann, T. Tamaoki, *Proc. Natl. Acad. Sci. USA* 80 (1983) 4604–4608.
- [2] G.I. Abelev, *Adv. Cancer Res.* 14 (1971) 295–358.
- [3] D.J. Brock, J.B. Scrimgeour, M.M. Nelson, *Clin. Genet.* 7 (1975) 163–169.
- [4] M. Seppala, *Ann. N.Y. Acad. Sci.* 259 (1975) 59–73.
- [5] E.A. Smuckler, M. Koplitz, S. Sell, *Cancer Res.* 36 (1976) 4558–4561.
- [6] L.R. Purves, I. Bersohn, E.W. Geddes, *Cancer* 25 (1978) 1261–1270.
- [7] E. Ruoslahti, M. Seppala, *Adv. Cancer Res.* 29 (1979) 275–346.
- [8] P.H. Lange, in: W.H. Fishman (Ed.), *Onco-Developmental Markers: Biological, Diagnosis and Monitoring Aspects*, Academic Press, New York, 1983, pp. 241–255.
- [9] H.F. Deutsch, *Adv. Cancer Res.* 56 (1991) 253–312.
- [10] M.S. Soloff, S.K. Swartz, F. Pearlmutter, K. Kithier, *Biochim. Biophys. Acta* 427 (1972) 644–651.
- [11] J. Uriel, B. de Nechaud, M. Dupiers, *Biochem. Biophys. Res. Commun.* 46 (1972) 1175–1180.
- [12] S. Nishi, H. Matsue, H. Yoshida, R. Yamamoto, M. Sakai, *Proc. Natl. Acad. Sci. USA* 88 (1991) 3102–3105.
- [13] D.C. Parmelee, M.A. Evenson, H.F. Deutsch, *J. Biol. Chem.* 253 (1978) 2114–2119.
- [14] J.C. Hsia, J.S. Er, C.T. Tan, T. Ester, E. Ruoslahti, *J. Biol. Chem.* 255 (1980) 4224–4227.
- [15] M. Nagai, J.D. Becker, H.F. Deutsch, *Oncodev. Biol. Med.* 3 (1982) 343–350.
- [16] E. Ruoslahti, T. Ester, M. Seppala, *Biochim. Biophys. Acta* 578 (1979) 511–519.
- [17] C.Y. Lu, P.S. Changelian, E.R. Unanue, *J. Immunol.* 132 (1984) 1722–1727.
- [18] J.M. Torres, J. Laborda, J. Naval, N. Darracq, M. Calvo, Z. Mishal, J. Uriel, *Mol. Immunol.* 26 (1989) 851–857.
- [19] J.L. Calwell, C.D. Severson, J.S. Thompson, *Fed. Proc. Fed. Am. Soc. Exp. Biol.* 32 (1973) 979.
- [20] M.D. Kirkitadze, N.V. Narizhneva, A.Yu. Tomashevski, S.A. Potekhin, V.N. Uversky, *Rus. J. Bioorgan. Chem. (Moscow)* 22 (1996) 353–356.

- [21] V.N. Uversky, N.V. Narizhneva, T.V. Ivanova, A.Yu. Tomashevski, *Biochemistry* 36 (1997) 13638–13645.
- [22] V.N. Uversky, N.V. Narizhneva, T.V. Ivanova, M.D. Kirkitadze, A.Yu. Tomashevski, *FEBS Lett.* 410 (1997) 280–284.
- [23] N.V. Narizhneva, T.V. Ivanova, A.Yu. Tomashevski, V.N. Uversky, *Mol. Biol. (Moscow)* 31 (1997) 1128–1133.
- [24] A.Yu. Tomashevski, N.V. Narizhneva, T.N. Melnik, V.N. Uversky, *Protein Pept. Lett.* 5 (1998) 295–301.
- [25] A.Yu. Tomashevski, T.N. Melnik, N.V. Narizhneva, M.M. Shavlovsky, V.B. Vasiliev, V.N. Uversky, *Protein Pept. Lett.* 6 (1999) 237–244.
- [26] T.P. King, E.M. Spencer, *Arch. Biochem. Biophys.* 153 (1972) 627–640.
- [27] J.R. Brown, *Fed. Proc. Fed. Am. Soc. Exp. Biol.* 34 (1975) 591.
- [28] D.Ya. Leybman, E.I. Tiktopulo, P.L. Privalov, *Biophysics (Moscow)* 20 (1975) 376–379.
- [29] K. Pedersen, *Scand. J. Clin. Lab. Invest.* 38 (1978) 659–667.
- [30] R.A. Bradshaw, W.T. Shearer, F.R.N. Gurd, *J. Biol. Chem.* 243 (1968) 3817–3825.
- [31] B. Sarkar, *Life Chem. Rep.* 1 (1983) 165–207.
- [32] F.R.N. Gurd, P.E. Wilcox, *Adv. Protein Chem.* 11 (1956) 311–427.
- [33] A.K. Nandedkar, C.E. Nurse, F. Friedbreg, *Int. J. Pept. Protein Res.* 5 (1973) 279–281.
- [34] T. Peters Jr., *Adv. Protein Chem.* 37 (1985) 161–245.
- [35] Y. Aoyagi, T. Ikenaka, F. Ichida, *Cancer Res.* 38 (1978) 3483–3486.
- [36] J.T. Wu, S.M. Monir-Vaghefi, F. Clayton, *Clin. Physiol. Biochem.* 5 (1987) 85–94.
- [37] B.L. Vallee, *Phys. Rev.* 39 (1959) 443–452.
- [38] E.J. Underwood, *Trace Elements in Human and Animal Nutrition*, Academic Press, New York, 1971.
- [39] J.F. Chlebowski, J.E. Coleman, in: H. Sigel (Ed.), *Metal Ions in Biological Systems*, Vol. 6, Marcel Dekker, New York, 1977, pp. 1–140.
- [40] H.E. Blum, P. Lehky, L. Kohler, E.A. Stein, E.H. Fischer, *J. Biol. Chem.* 252 (1977) 2834–2838.
- [41] M.R. Eftink, C.A. Ghiron, *Anal. Biochem.* 114 (1981) 199–227.
- [42] K.A. Oberg, A.L. Fink, *Anal. Biochem.* 256 (1998) 92–106.
- [43] V. Cabiliaux, K.A. Oberg, P. Pancoska, T. Walz, P. Agre, A. Engel, *Biophys. J.* 73 (1997) 406–417.
- [44] K.A. Oberg, J.M. Ruysschaert, M. Azarkan, N. Smolders, S. Zerhouni, R. Wintjens, A. Amrani, Y. Looze, *Eur. J. Biochem.* 258 (1998) 214–222.
- [45] P.L. Privalov, S.A. Potekhin, *Methods Enzymol.* 131 (1986) 4–51.
- [46] R.W. Sarver Jr., W.C. Krueger, *Anal. Biochem.* 199 (1991) 61–67.
- [47] V.N. Uversky, N.V. Narizhneva, *Biochemistry (Moscow)* 63 (1998) 420–433.
- [48] R. Vogel, G.-B. Fan, M. Sheves, F. Siebert, *Biochemistry* 40 (2001) 483–493.
- [49] E.A. Permyakov, *Calcium Binding Proteins*, Nauka, Moscow, 1993.
- [50] E.J. Cohn, J.T. Edsall, *Proteins, Amino Acids and Peptides as Ions and Dipolarizations*, Reinhold, New York, 1942.